Voltage-Clamped Class-E Inverter With Harmonic Tuning Network for Magnetron Drive

Young-Jin Woo, Sang-Kyung Kim, and Gyu-Hyeong Cho, *Member, IEEE*

***Abstract*—A passive lossless snubber utilizing harmonic resonance is proposed for the voltage-driven class-E inverter. This snubber reduces the peak resonant voltage stress across the switch in class-E operation by adding the third-order harmonic current into the fundamental resonant part and can be extended to a higher-order network for further reduction. Though the principle is actually equivalent to the class-F operation in RF power amplifiers, it is first tried for the class-E inverter without a current source inductor. A series of analyses is performed to find component values that provide the optimum harmonic condition, and the experimental results from the inverter power supply for driving a magnetron are presented.**

***Index Terms*—Class E, class F, harmonic resonance, induction heating (IH), microwave oven (MWO), snubbers.**

I. Introduction

A single-ended quasi-resonant zero-voltage switching (ZVS) inverter with a single insulated gate bipolar transistor (IGBT) is usually adopted to drive a magnetron for household microwave ovens (MWOs) nowadays. This actually class-E inverter power supply has been evolved from a ferroresonant step-up transformer to reduce size and weight and to control the output power for smart cooking [1]. This type of class-E inverter is also the main topology for the now popular induction heating (IH) appliances, which have many advantages over those using conventional heating [2].

As exhibited by the class-E operation in power amplifiers, which was first introduced in [3], class E features inherent soft switching, hence, small switching loss, and simple single-switch configuration. Though throughout years, most of the works related to class-E have been done on the configuration with a current source inductor in the dc-feed line [3]–[6], the circuit becomes simpler and more cost effective if more harmonics are acceptable in their outputs. This class-E circuit is realized with only one inductor and one capacitor in the load network [7], [8]. The aforementioned MWO and IH seem to be the successful applications of this type of class-E operation to power conversion. In the RF field, main discussions are found on its optimum operating condition—zero-voltage switch and zero-voltage slope at the instant the switch is turned on. In inverter applications, however, zero-voltage slope is usually unimportant, whereas ZVS is crucial to the switching losses.

Manuscript received July 21, 2005; revised May 4, 2006. This work was supported by the Ministry of Commerce, Industry and Energy, Korea. This paper was recommended by Associate Editor W.-H. Ki.

The authors are with the Department of Electrical Engineering and Computer Science, Korea Advanced Institute of Science and Technology, Daejeon 305-701, Korea (e-mail: youngjin.woo@kaist.ac.kr).

Digital Object Identifier 10.1109/TCSII.2006.884121

This simple and cost-effective inverter does operate well for a 100-V ac line, but its high peak voltage across the switch in resonance is a potential problem, making it difficult to use for higher ac line voltages. The peak voltage is about four times higher than the input dc voltage when satisfying ZVS condition. Thus, other inverter topologies have been proposed to resolve this problem. Good examples of such are the active clamp class-E (ACCE) inverter [2], [9] and the half-bridge-type series resonant inverter [10]. However, the adoption of these topologies raises the inverter cost due to the high price of the additional power switch.

In contrast to these two-switch approaches, other class-E variants with a passive voltage clamping feature have been recently proposed for power amplifiers [11]–[13]. However, they are not acceptable for large power inverters, especially for the voltage-driven class-E inverters with a loosely coupled leakage transformer specifically used for driving a magnetron.

In this brief, a passive lossless snubber utilizing harmonic resonance is proposed, which makes it possible to sustain the low-cost single-switch class-E inverter in driving a magnetron. Though the idea was inspired by the Fourier series expansion of a square wave, it is actually found in radio engineering as a class-F or a higher-order class-E power amplifier [14], [15]. However, it has not been tried yet in power conversion, especially with this type of class-E inverter that does not have a current source inductor—RF choke. To construct the snubber network that gives the optimum harmonics, the theoretical groundwork is first accomplished as a general form, and then, simulation and experimental results are presented to validate the reasoning.

II. System Overview

MWOs are the high-voltage systems that generate microwave energy that cooks food. The heart of the system is the magnetron, which produces the required 2.45-GHz microwave. The configuration of the inverter power supply for driving the magnetron is shown in Fig. 1, with key operational waveforms at each part.

The input ac line voltage is rectified by the diode bridge and the LC filter. The rectified dc voltage fluctuates as high as the ac line amplitude since the purpose of the filter is to remove switching frequency noise. The main power stage is the voltage source type of class-E inverter, which is the most efficient inverter known so far. The on time of the IGBT switch is controlled mainly for power factor correction (PFC) and partly to limit the peak power and the peak resonant voltage. Consequently, its duty and frequency change according to the dc bus voltage $V_{\rm dc}$. The switching frequency decreases in its valley region and increases in its peak region, but it does not normally

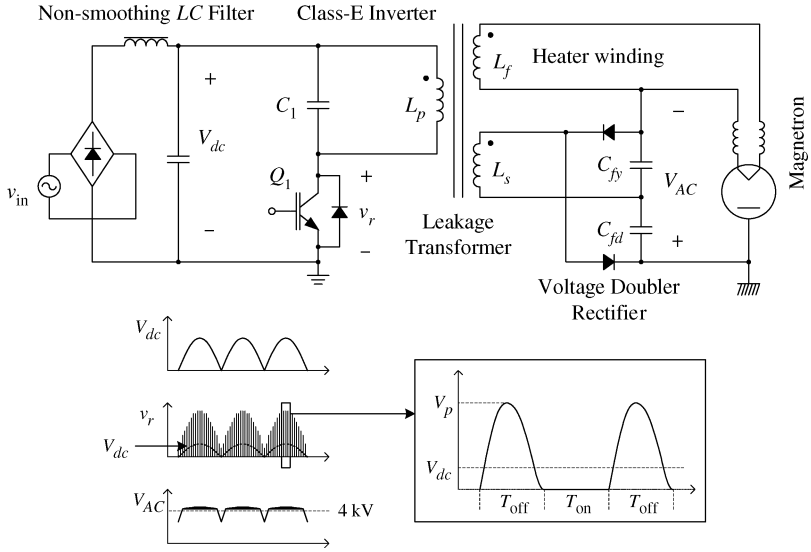

Fig. 1. Configuration of the class-E inverter power supply driving the magnetron.

exceed 50 kHz because of the reliability degradation with an increased switching loss in the IGBT. The step-up transformer boosts the inverted voltage, and the secondary diodes and capacitors constitute a voltage doubler rectifier. The induced high dc voltage drives the magnetron. When the voltage between the anode and the cathode exceeds about 4 kV, the magnetron anode current begins to flow from the anode to the cathode. On the other hand, when the voltage between the anode and the cathode is lower than a certain cutoff voltage, the anode current mostly does not flow. Hence, the electrical equivalent circuit model of the magnetron can be simply represented by a Zener diode.

The efficiency of the system is estimated by boiling water in the MWO and measuring the temperature rise. The main energy loss occurs in the magnetron whose efficiency is around 80%.

III. Configuration and Operation Principle

The class-E inverter core is composed of an IGBT switch Q_1, a resonant capacitor C_1, and a step-up high-voltage transformer T_1 with a loose coupling factor k_c. When Q_1 is on, power is transferred to the magnetron by forward operation. Next, when Q_1 is off, C_1 resonates with the equivalent inductance L_1 of the transformer side, and power is transferred by flyback manner. Furthermore, when the resonant voltage across the switch v_r drops to zero, Q_1 turns on again, and the above cycle goes on and on. Since the switch current and voltage waveforms do not overlap during the switching time intervals, switching losses are virtually zero, yielding high efficiency. The input power is controlled by the on time of Q_1, which actually determines the input current waveform and, hence, the power factor. A power factor near unity is obtained by controlling the on time, which is similar to the boost PFC scheme.

The proposed snubber is actually the harmonic tuning network shown in Fig. 2(b). It incorporates single or multiple harmonic branches into the original class-E inverter circuit. Each branch connected parallel to C_1 is composed of a inductor L_k, a capacitor C_k, and a diode D_k. The dominant current component in each branch, which is denoted by i_k, flows through C_1.

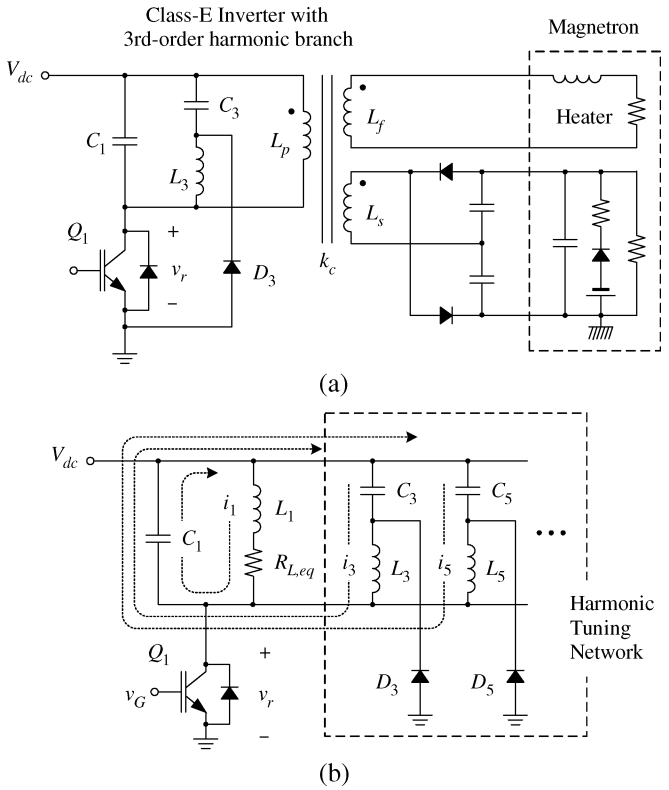

Fig. 2. (a) Class-E inverter with the proposed snubber. (b) Generalized representation of the proposed snubber with the ac equivalent core of the class-E inverter.

In case only the third harmonic branch is configured ($m = 1$ and $k = 3$) as shown in Fig. 2(a), when Q_1 is off, the third harmonic current mainly flows through C_1, concurrently with the fundamental current. In addition, it operates oppositely around the resonant peak, hence, resulting in the reduced peak voltage. D_3 prevents the harmonic resonance from continuing during the switch-on time, and the residual current in L_3 freewheels through Q_1 and D_3.

If the higher harmonic branches are further added, a lower peak voltage can be obtained. In each branch, the resonant frequency ω_{0k} and the characteristic impedance Z_k, which are defined in the follows, should be properly determined to lower the peak value of v_r under the same output power condition:

$$\omega_{0k} = 1/\sqrt{L_k C_k} \quad Z_k = \sqrt{L_k/C_k}.$$

The proposed snubber does operate without D_k's. However, that makes the snubber more sensitive to the input line or power variation, because the consequent on time change directly affects the relationship between the fundamental and the harmonics, from which rather disastrous result may come.

IV. Formulation

Intuitively or by solving the $2(m+1)$th-order differential equation, during the resonant period, v_r can be expressed as

$$v_r(t) = V_{\rm dc} + \sum_{k=1}^{2m+1} V_k \sin \omega_k t. \tag{1}$$

The expression is rather simplified as follows: It is a damped oscillatory system, and therefore, it would be natural to encompass exponential terms, but this is neglected in (1). The operation of the voltage doubler, which is used for the magnetron drive, results in the secondary side resonance. This affects the primary side resonances and complicates the whole operation, but the effect is not dominant and was also neglected in this formulation. Furthermore, it sometimes happens that the harmonic currents leak through the freewheeling diodes out of the resonant tank even during the switch-off time. It also makes the derivation less ideal, but the duration is short enough for most cases.

First, ω_k should satisfy the condition $\omega_k = k \cdot \omega_1$ to make an odd harmonic series. Second, The relative magnitudes of V_k's compared with V_1 can be determined from the following reasoning: When the Fourier series coefficients of a square wave are used, the waveform converges too slowly as m increases, which is an important point in physical realization, and has an undesirable effect known as the Gibbs phenomenon. If only the third harmonic component is used $(m = 1)$, a coefficient between 1/6 and 1/9 is a better choice, not 1/3. The minimum peak is obtained at 1/6, and the flat-top waveform is achieved at 1/9. When more harmonics are used $(m \geq 2)$, the peak reduces further, but the coefficients are not easily determined theoretically. One particular result with $m = 2$, however, is still obtainable—the flat-top waveform at 1/6 for the third harmonic and 1/50 for the fifth harmonic, as was already noticed in [16].

Equation (1) can be represented as the summation of each harmonic current at C_1, i.e.,

$$v_r(t) = V_{\rm dc} + \frac{1}{C_1} \int_0^{\pi/\omega_1} \sum_{k=1}^{2m+1} \omega_k C_1 V_k \cos \omega_k t \, dt. \tag{2}$$

Recognizing that each branch current i_k is almost equal to the term of $\omega_k C_1 V_k \cos \omega_k t$, (2) shows that the current ratio of i_k to i_1 should be k times the ratio of V_k to V_1. Then, the relative magnitudes of Z_k's should be determined correspondingly to organize the optimum harmonic mixing.

To easily understand the relations between the fundamental and the harmonics as well as for the convenience of design, the following normalized values of ω_{0k} and Z_k are preferred:

$$n_{\omega_k} = \frac{\sqrt{L_1 C_1}}{\sqrt{L_k C_k}} \quad n_{Z_k} = \frac{\sqrt{L_k/C_k}}{\sqrt{L_1/C_1}}.$$

Then, the values of L_k and C_k are defined as follows:

$$L_k = \frac{L_1}{n_{\omega_k}} n_{Z_k} \quad C_k = \frac{C_1}{n_{\omega_k} n_{Z_k}}.$$

The use of primary inductance L_p of T_1 is, however, more preferable since the equivalent inductance L_1 is not easily available in real design. If we define another factor of α as $L_1 = \alpha \cdot L_p$, α is approximately $(1 - k_c^2)$ for most of the dc bus voltage $V_{\rm dc}$ fluctuation. When $V_{\rm dc}$ is low, i.e., in the valley region, there are time periods when the secondary current of T_1 does not flow, and therefore, the voltage doubler circuit operates in discontinuous mode. As a result, α somewhat increases equivalently, and the harmonics are established away from the optimum condition. However, it matters little since the resonant voltage level V_p in the valley region is low enough. For the purpose of easy manipulation of data, by letting α be unity, the relationships described above are redefined as follows:

$$N_{\omega_k} = \frac{\sqrt{L_p C_1}}{\sqrt{L_k C_k}} \quad N_{Z_k} = \frac{\sqrt{L_k/C_k}}{\sqrt{L_p/C_1}}$$
$$L_k = \frac{L_p}{N_{\omega_k}} N_{Z_k} \quad C_k = \frac{C_1}{N_{\omega_k} N_{Z_k}}.$$

Now, we can guess the initial design values for the optimum harmonic condition under the simplifying assumptions, though the reasoning should be concluded with SPICE simulation. Roughly regarded as ω_{0k}, each ω_k actually deviates from ω_{0k} by the influence of the other branches, which has the form of a function of all ω_{0k}'s and Z_k's referring to the solution of the differential equation.

For $m = 1$, together with $\omega_3 = 3 \cdot \omega_1$, the following equations are obtained:

$$\omega_1^2 + (3\omega_1)^2 = \omega_{01}^2 \cdot \left(1 + \frac{n_{\omega_3}}{n_{Z_3}} + n_{\omega_3}^2\right) \tag{3}$$
$$\omega_1^2 \cdot (3\omega_1)^2 = \omega_{01}^4 \cdot n_{\omega_3}^2. \tag{4}$$

From (1) and (2), with the assumptions that the fundamental current is dominant in L_1 and that v_r has a flat-top waveform, we arrive at the following relationship:

$$\frac{V_3}{V_1} = 1 - \frac{\omega_1^2}{\omega_{01}^2} = \frac{1}{9}. \tag{5}$$

Substituting (5) into (3) and (4) gives a solution of $n_{\omega_3} = 2.67$ and $n_{Z_3} = 3.43$. It corresponds to N_{ω_3} of 4.18 and N_{Z_3} of 2.19 when k_c of T_1 is 0.77. In reality, further tradeoffs are possible in determining the values of L_k and C_k, considering the ratings of D_k's.

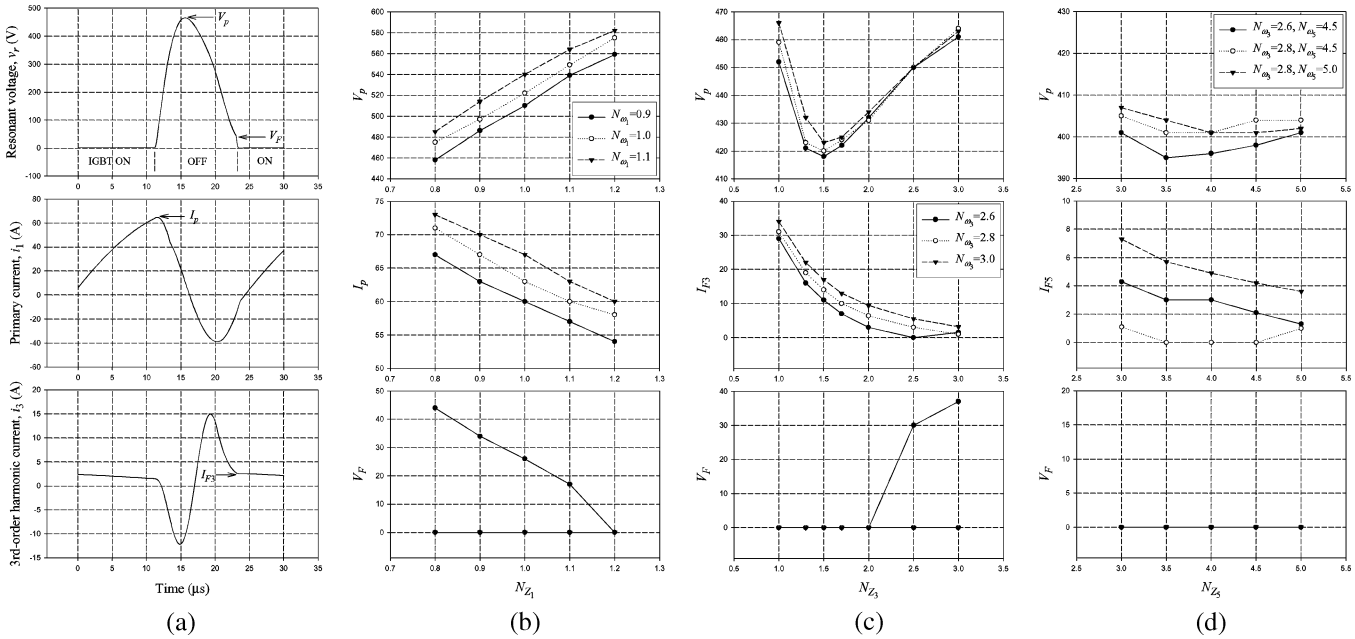

Fig. 3. (a) Sample waveforms with key parameters under a nonoptimum harmonic mixing. (b)–(d) Characteristics varied with N_{Z_k} and N_{ω_k}. $V_{\rm dc} = 140$ V, $P_{\rm in} = 2.5$ kW, $k_c = 0.77$, $L_p = 36.5$ μH, $L_s = 13.4$ mH, $L_f = 0.25$ μH, $C_1 = 0.33$ μF, $C_{fy} = 6$ nF, and $C_{fd} = 3$ nF. (b) Basic inverter characteristics around the default value of L_p and C_1. (c) First-order harmonic tuning network ($m = 1$). (d) Second-order harmonic tuning network ($m = 2$) with $N_{Z_3} = 1.5$.

V. Simulation and Experimental Results

Using PSPICE simulation, the operation of the proposed snubber was confirmed, and their characteristics were measured and analyzed. Simulation models of IGBTs were created, referring to Fairchild models of 1000-V/60-A and 900-V/60-A IGBTs and their data sheets. More accurate models can be made, but it complicates the work and tends to cause convergence problem in the circuit simulation. The equivalent circuit model parameters of the magnetron in Fig. 2(a) were determined by matching the simulation waveforms with the actual ones. Major concerns are the variation of resonant peak voltage V_p and current I_p, freewheeling current I_{Fk} at each diode in harmonic branches, and ZVS failure voltage V_F according to the values of L_k and C_k. They are illustrated in Fig. 3(a). V_F is the voltage across the switch when it turns on—Q_1 turns on with some time delay after v_r crosses over a predefined value. The results are plotted versus N_{Z_k} for several values of N_{ω_k} under the same input power as shown in Fig. 3(b)–(d). Without the proposed snubber, as Fig. 3(b) shows, V_p cannot be lowered much because it is inversely proportional to V_F. The added harmonics do not have much effect on I_p and are, hence, omitted in Fig. 3(c) and (d). Near-optimum values of N_{ω_3} and N_{Z_3} for the minimum V_p are found as 2.6 and 1.5, respectively, for $m = 1$. Rather lower values, compared with the theoretically expected values, could be mainly attributed to the lowered slope of the fundamental current around the peak region of v_r by the load effect—more accurately, the secondary resonance. Fig. 3 shows that the peak stress can be reduced by about 23% without ZVS failure for $m = 2$.

The efficiency of the inverter little changes with the adoption of the proposed snubber. Our simulation result shows that the efficiency reduces to 92.0% from 92.8% under the same input power of 1.3 kW when only the third-order harmonic branch

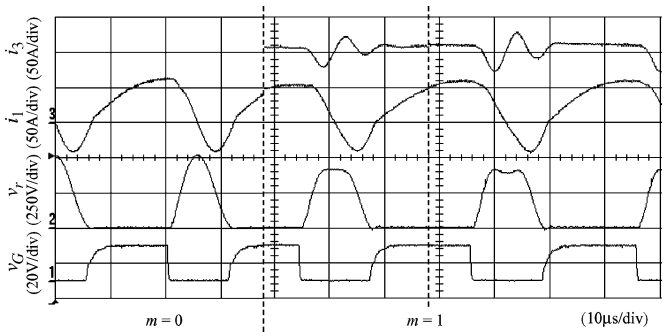

Fig. 4. Measured waveforms at the peak of the dc bus voltage. $V_{\rm in} = 100 V_{\rm ac}$, $P_{\rm in} = 1.3$ kW, $P_{\rm in,pk} \approx 2.5$ kW, $L_p = 36.5$ μH, $L_s = 13.4$ mH, $L_f = 0.25$ μH, $C_1 = 0.33$ μF, $k_c = 0.77$, $C_{fy} = 6$ nF, and $C_{fd} = 3$ nF; $N_{\omega_3} = 2.6$ and $N_{Z_3} = 1.8$ ($L_3 = 24.1$ μH and $C_3 = 69$ nF); and $N_{\omega_3} = 2.6$ and $N_{Z_3} = 1.5$ ($L_3 = 21.2$ μH and $C_3 = 84.5$ nF).

was constituted near the optimum condition. A sine wave of 100 V/60 Hz was applied to the input diode bridge, and the power consumption at the equivalent magnetron model was measured as the output power. The ZVS and PFC controllers were also implemented in the circuit level, which is actually the same as in the experimental setup. A default diode model in PSPICE was used for the input bridge rectifier and the high-voltage diodes in the voltage doubler rectifier. A built-in diode model in the Fairchild IGBT model was used for the diodes D_k's in the harmonic tuning network. Series resistances of the transformer windings were neglected.

Fig. 4 shows the experimental result under the following conditions: ac line input of 100 V, input power of 1.3 kW, input peak power of 2.5 kW, and power factor of about 0.98. The SGL60N90DG3, a 900-V/60-A Fairchild IGBT device, was used as the main switch. The turn ratio of the three-winding high-voltage transformer is $N_p : N_s : N_f = 16 : 310 : 1$. The

switching frequency changes roughly from 50 kHz in the peak region to 20 kHz in the valley region of the dc bus voltage. The operational waveforms of the basic class-E inverter with only the fundamental component is shown in the left part of the figure. The remaining two figures show the changed waveforms after the third-order harmonic component is added ($m = 1$). The middle part of the figure shows that the harmonic mixing is near optimum ($N_{\omega_3} = 2.6$ and $N_{Z_3} = 1.8$), and the right part of the figure shows that the third-order harmonic current is excessive ($N_{\omega_3} = 2.6$ and $N_{Z_3} = 1.5$). Notice that i_3 shows the opposite slope to i_1 around the v_r peak region. Compared with the original waveform, the peak voltage is lowered by about 20%.

One drawback with this snubber in reality comes from an extremely stiff nonlinear characteristic of the magnetron, particularly before and after it starts. The input average power is slightly over 100 W before it starts and up until the anode-to-cathode voltage V_{AC} reaches about 8 kV. It starts within a few seconds, and then it acts like a Zener diode in the normal operation mode. Hence, the value of L_1 varies approximately from L_p to $(1-k_c^2)L_p$ before and after the magnetron starts, which deviates the harmonics from the optimum condition. In IH applications, the proposed harmonic mixing can be free from this problem.

VI. Conclusion

The proposed harmonic tuning network is simply configured and effectively reduces the resonant peak voltage stress of the voltage-driven class-E inverter. It uses only low-cost passive elements instead of a costly IGBT, compared with an active clamp or a half-bridge approach, and is free from the troublesome work of floating gate control. To find the optimum harmonic condition, basic mathematical reasoning was followed by intensive computer simulation up to the second order, which is thought be a practically useful range. It was successfully tested for the magnetron drive and could find other applications based on this voltage source type of class-E operation.

Acknowledgment

The authors would like to thank B. Arlt of the PCIM for his cheerful help.

References

[1] S. Yamaguchi, S. Matsubayashi, H. Kako, and R. Narita, "Compact inverter power supply for microwave oven by new switching device IGBT," in *Proc. PCIM Europe*, Jun. 1990, pp. 267–278.

[2] D.-Y. Lee and D.-S. Hyun, "Hybrid control scheme of active-clamped class E inverter with induction heating jar for high power applications," *Proc. Inst. Electr. Eng.—Electr. Power Appl.*, vol. 151, no. 6, pp. 704–710, Nov. 2004.

[3] N. O. Sokal and A. D. Sokal, "Class E—A new class of high efficiency tuned single-ended switching power amplifiers," *IEEE J. Solid-State Circuits*, vol. SSC-10, no. 3, pp. 168–176, Jun. 1975.

[4] F. H. Raab, "Idealized operation of the class-E tuned power amplifier," *IEEE Trans. Circuits Syst.*, vol. CAS-24, no. 12, pp. 725–735, Dec. 1977.

[5] M. K. Kazimierczuk and K. Puczko, "Exact analysis of class E tuned power amplifier at any Q and switch duty cycle," *IEEE Trans. Circuits Syst.*, vol. CAS-34, no. 2, pp. 149–159, Feb. 1987.

[6] M. K. Kazimierczuk and D. Czarkowski, *Resonant Power Converters*. New York: Wiley-Interscience, 1995.

[7] N. O. Sokal, "Class E high-efficiency switching-mode tuned power amplifier with only one inductor and one capacitor in load network—approximate analysis," *IEEE J. Solid-State Circuits*, vol. SSC-16, no. 4, pp. 380–384, Aug. 1981.

[8] M. Kazimierczuk, "Exact analysis of class E tuned power amplifier with only one inductor and one capacitor in load network," *IEEE J. Solid-State Circuits*, vol. SSC-18, no. 2, pp. 214–221, Apr. 1983.

[9] T. Matsushige, E. Miyata, M. Ishitobi, M. Nakaoka, D. Bessyo, K. Yasui, I. Hirota, and H. Omori, "Voltage-clamped soft switching PWM inverter-type DC–DC converter for microwave oven and its utility AC side harmonics evaluations," in *Proc. 3rd Int. Power Electron. and Motion Control Conf.*, Aug. 2000, vol. 1, pp. 147–152.

[10] M. Ishitobi, S. Moisseev, L. Gamage, M. Nakaoka, D. Bessyo, and H. Omori, "Pulse width and pulse frequency modulation pattern controlled ZVS inverter type AC–DC power converter with lowered utility AC grid side harmonic current components for magnetron drive," in *Proc. Conf. Rec. IEEE-PESC*, Jun. 2002, vol. 4, pp. 2062–2067.

[11] T. Suetsugu and M. K. Kazimierczuk, "Design procedure for lossless voltage-clamped class E amplifier with a transformer and a diode," *IEEE Trans. Power Electron.*, vol. 20, no. 1, pp. 56–64, Jan. 2005.

[12] ——, "Voltage clamped class-E amplifier with Zener diode," *IEEE Trans. Circuits Syst. I, Fundam. Theory Appl.*, vol. 50, no. 10, pp. 1347–1349, Oct. 2003.

[13] ——, "Voltage-clamped class E amplifier with transmission-line transformer," in *Proc. IEEE Int. Symp. Circuits and Syst.*, May 2005, vol. 1, pp. 712–715.

[14] F. H. Raab, "Class-E, class-C, and class-F power amplifiers based upon a finite number of harmonics," *IEEE Trans. Microw. Theory Tech.*, vol. 49, no. 8, pp. 1462–1468, Aug. 2001.

[15] S. D. Kee, I. Aoki, A. Hajimiri, and D. Rutledge, "The class-E/F family of ZVS switching amplifiers," *IEEE Trans. Microw. Theory Tech.*, vol. 51, no. 6, pp. 1677–1690, Jun. 2003.

[16] F. H. Raab, "Class-F power amplifiers with maximally flat waveforms," *IEEE Trans. Microw. Theory Tech.*, vol. 45, no. 11, pp. 2007–2012, Nov. 1997.